fibers

MDPI

Article

A Method to Process Hollow-Core Anti-Resonant Fibers into Fiber Filters

Xiaosheng Huang, Ken-Tye Yong and Seongwoo Yoo *

School of Electrical and Electronic Engineering, The Photonics Institute, Nanyang Technological University, 50 Nanyang Avenue, Singapore 639798, Singapore; xhuang012@e.ntu.edu.sg (X.H.); ktyong@ntu.edu.sg (K.-T.Y.)
* Correspondence: seon.yoo@ntu.edu.sg; Tel.: +65-6592-7597

Received: 25 July 2018; Accepted: 15 August 2018; Published: 22 November 2018

Abstract: Hollow-Core Anti-Resonant Fiber (HC-ARF) shows promising applications. Nevertheless, there has been a persistent problem when it comes to all-fiber integration due to a lack of HC-ARF-based fiber components. In response to this remaining challenge, we investigate a reliable, versatile and efficient method to convert an HC-ARF into a fiber filter. By locally heating an HC-ARF with a CO_2 laser, the fiber structure becomes deformed, and cladding capillaries shrink to produce a thicker wall. This process is analogous to "writing" a new fiber with a thicker wall on the original fiber, resulting in creating new high loss regions in the original transmission bands. Thus, the construction of a fiber filter is realized by "writing" a new fiber on the original fiber. The feasibility of this method is confirmed through experiments, adopting both one- and two-layer HC-ARF. The HC-ARF-based fiber filters are found to have transmission spectra consistent with simulation prediction. Both band pass and band reject fiber filters with more than a 20-dB extinction ratio are obtainable without extra loss. Thus, an in-fiber HC-ARF filter is demonstrated by the CO_2 writing process. Its versatile approach promises controlled band selection and would find interesting applications to be discussed.

Keywords: fiber filters; hollow core fibers; anti-resonant; photonic crystal fibers; fabrication

1. Introduction

Since the first theoretical demonstration in 1995 [1], Hollow-Core Photonic Crystal Fibers (HC-PCFs), as a remarkable breakthrough in fiber optics, have made it possible to guide light in the air core. This unique guiding property promises the potentials of achieving a higher damage threshold, lower Rayleigh scattering, lower material absorption and lower nonlinearity as compared to conventional fibers [2]. Hence, HC-PCFs have promising applications in areas of high power/ultrafast beam delivery [3], pulse compression [4] and communication systems [5], to name a few. One type of HC-PCFs is Hollow-Core Photonic Bandgap Fibers (HC-PBGFs), the record loss of which is 1.2 dB/km at 1.62 μm [6]. The HC-PBGF typically has a relatively narrow transmission band. The other type of HC-PCF is the so-called Hollow-Core Anti-Resonant Fibers (HC-ARFs), the guiding property relies of which on the combination of anti-resonance and inhibited coupling to low density of states cladding modes [7,8]. The HC-ARF has received ever-increasing interest thanks to its multiple broad transmission bands [7,9], simple and flexible cladding structures [10–13] and relatively low transmission loss [8,14–16]. The HC-ARFs show promising prospects in applications such as delivering light with a wide spectral range from ultra violet to mid-infrared [17,18], an optofluidic system [19,20] and light gas interaction [21]. Despite the unique properties of hollow core fibers, their connectivity to conventional fiber components is inefficient due to the mismatch of numerical aperture, as well as core size. As a result, most of the HC-ARF-based optical systems rely on free space optical components that hinder the wide uptake of hollow core fibers at the system level.

An alternative to the attempt of connecting hollow core fibers to solid fiber-based components is to develop HC-ARF-based fiber components. Such hollow core-based components definitely facilitate the simplification of the HC-ARF-based optical system. To date, the reported works on hollow-core fiber-based components are limited, with most of them focusing on fiber couplers [22–24]. Fiber filters, on the one hand, comprise one of the most important fiber-based components that allows the transmission of certain wavelengths [25,26]. Nonetheless, the realization of hollow core-based filters has not yet been demonstrated. In fact, HC-ARFs are of great potential to be fiber filters on account of the core wall thickness-dependent transmission wavelengths and transmission bandwidth. Combining HC-ARFs with different core wall thicknesses will enable customization of the actual transmission bands.

In this work, we report a reliable, flexible and efficient method to process HC-ARFs into fiber filters. By locally heating an HC-ARF with a CO_2 laser, the fiber structure becomes deformed, and cladding capillaries shrink to have thicker walls. This process is analogous to "writing" a new fiber with a thicker wall on the original fiber, resulting in creating new high loss regions (resonant wavelengths) in the original transmission bands. Thus, the control of the transmission wavelengths of the fiber filter is realized by controlling the wall thickness "written" on the original fiber. Furthermore, this method is able to integrate an in-line fiber filter into an HC-ARF without extra loss and is promising in many HC-ARF-based applications, which are also discussed.

2. Methods

As depicted in Figure 1a, the HC-ARF is composed of one layer of capillaries that surrounds the hollow region to form an anti-resonant guidance. The nodeless cladding and negative curvature of the core-cladding boundary are two critical features of HC-ARF that significantly reduce the fiber loss [13,27,28]. The HC-ARF fabricated by the stack and draw technique [9,29] has a good structure, as presented in Figure 1b. Among all the geometric parameters, the most important parameters are core diameter D, capillary size p and capillary wall thickness t. While both D and p relate to the fiber loss, t is the only geometric parameter that determines the transmission wavelengths. Transmission bands of HC-ARFs are determined by the resonant wavelengths. Resonant wavelengths are the central wavelength of high loss regions, and a low loss transmission band exists between every adjacent high loss region. The m-th order resonant wavelength, λ_m, can be calculated from the following equation [30]:

$$\lambda_m = \frac{2t \times \sqrt{{n_2}^2 - n_1^2}}{m}, m = 1, 2, 3... \quad (1)$$

where t is the wall thickness, n_2 is the refractive index of cladding material and n_1 is the refractive index of core material. In the case of silica-based air core fiber, we set $n_2 = 1.45$ and $n_1 = 1.00$. The low loss region between the m-th and $(m+1)$-th resonant wavelengths is called the m-th transmission band.

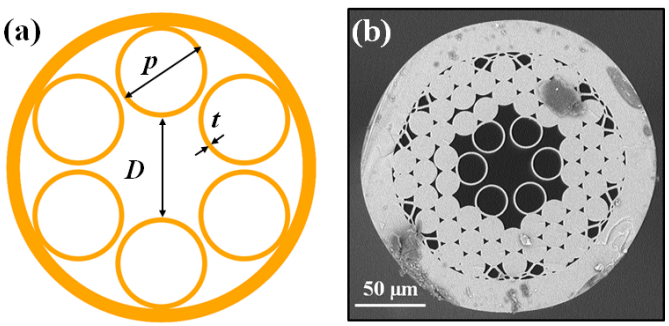

Figure 1. (**a**) Schematic diagram of the cross-sectional view of a negative curvature HC-ARF (Hollow-Core Anti-Resonant Fiber). t is the capillary wall thickness; p is the capillary outer diameter; and D is the core diameter. (**b**) HC-ARF fabricated by the stack and draw method that produces a good structure.

The second and third transmission bands of HC-ARFs with different wall thicknesses are studied by simulation. The results are calculated by a vector wave expansion method using the open source software Polymode [31]. As shown in Figure 2a, combing a fiber ($t = 1.0$ μm) to another fiber possessing a thicker wall ($t = 1.1$ μm) leads to the narrowing of transmission bands. We define the transmission band when its CL is below 3 dB/m. If the wall thickness difference between the fibers becomes larger (e.g., $t = 1.0$ μm and $t = 1.2$ μm), the $(m+1)$-th transmission band of the thick-wall fiber can overlap with the m-th transmission band of the thin-wall fiber, resulting in multiple and narrow transmission bands (see Figure 2b).

Although combing HC-ARFs with different t can narrow the transmission bands, it is inefficient and troublesome to fabricate multiple HC-ARFs with different wall thicknesses and to splice them together. Instead, it makes more sense to process a piece of uniform fiber to have varied wall thicknesses along its axis. To achieve this, a CO_2 laser-assisted glass processing stage (LZM-100 from Fujikura Ltd., Tokyo, Japan) is used to process the fiber. As illustrated in Figure 3a, a piece of HC-ARF is loaded onto two fiber holders. During the fiber processing, both holders rotate at the same speed to ensure symmetric heating. In parallel, the holders longitudinally move at the same traveling speed toward the same direction in order to avoid any twist or stretch. A section of the HC-ARF is locally heated by the CO_2 laser with tunable power P. Under the CO_2 laser treatment, the exposed section undergoes shrinkage due to surface tension, resulting in increasing wall thickness. The wall thickness of the processed fiber is controllable by adjusting the laser power P. Hence, uniform modification of wall thickness is achievable by moving the laser exposure along the fiber axis, as illustrated in Figure 3b.

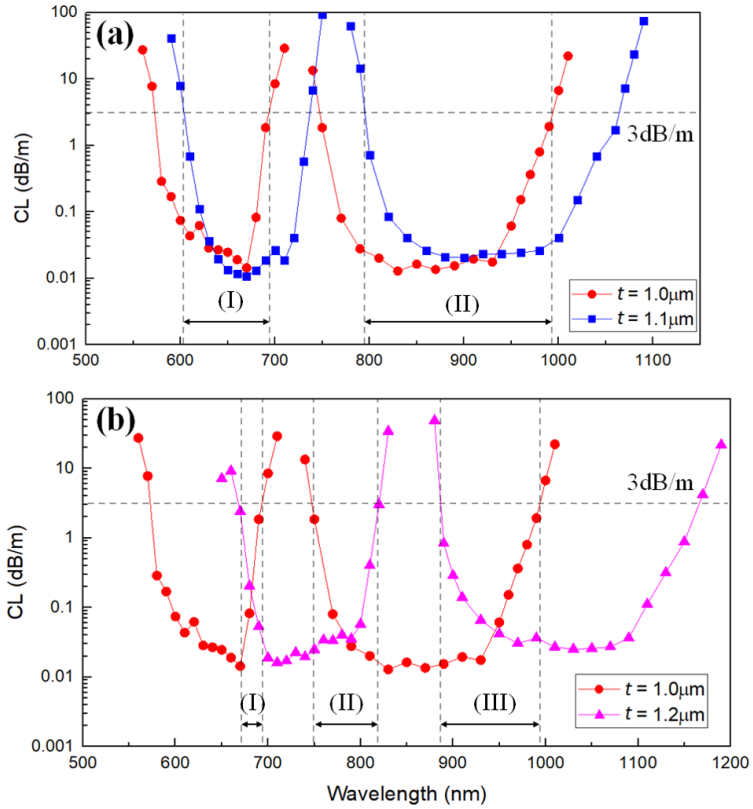

Figure 2. Simulated second and third transmission bands of HC-ARFs with different t. Roman numerals mark the hybrid transmission bands of HC-ARFs with: (**a**) $t = 1.0$ μm and $t = 1.1$ μm; (**b**) $t = 1.0$ μm and $t = 1.2$ μm. In all cases, $D = 30.0$ μm, $p = 24.0$ μm.

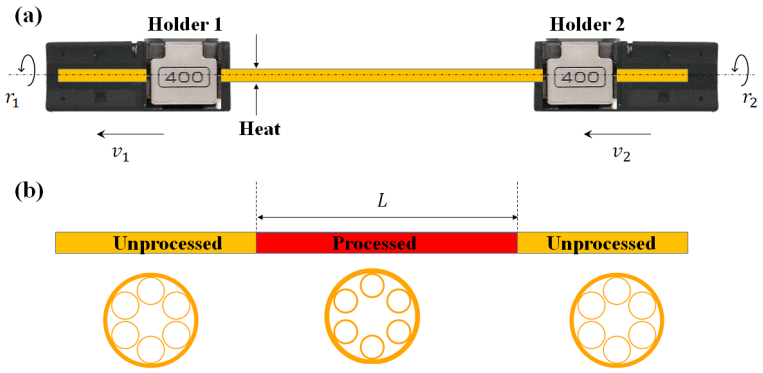

Figure 3. (**a**) Schematic diagram of the HC-ARF processing, $r_1 = r_2 = 50$ rpm, $v_1 = v_2 = 0.5$ μm/ms; heating is realized with a CO_2 laser. (**b**) During the process, the HC-ARF undergoes structural deformation, yielding a thicker wall. L is the length of the processed fiber.

3. Results and Discussion

A 17-cm HC-ARF, Fiber #1 (please, see Figure 4), was processed with the aforementioned method under different heating powers. The original fiber (Fiber #1) had a wall thickness $t = 1.40$ μm and a core diameter $D = 31.2$ μm, while the wall thickness of the processed fiber increased to be 1.49 μm (Fiber #2, processed with 19.2 W of heating power) and 1.63 μm (Fiber #3, processed with 20.1 W of heating power), respectively. As predicted, under high temperature, capillaries shrunk to induce a thicker wall due to surface tension. Transmission spectra of different fiber combinations were also measured, as shown in Figure 4. Resonant wavelengths of Fiber #2 and Fiber #3 were calculated and marked with blue and red dashed lines, respectively. As demonstrated by the measured transmission spectra, writing a new fiber on the original fiber by the CO_2 laser introduced a new high loss region (extra resonant band), realizing a selective transmission/rejection in-fiber filter. We noticed that the writing process did not introduce any significant extra loss. Besides the controllability, the reproducibility of the proposed method was also verified as the fibers processed under the same CO_2 laser power showed similar transmission spectra.

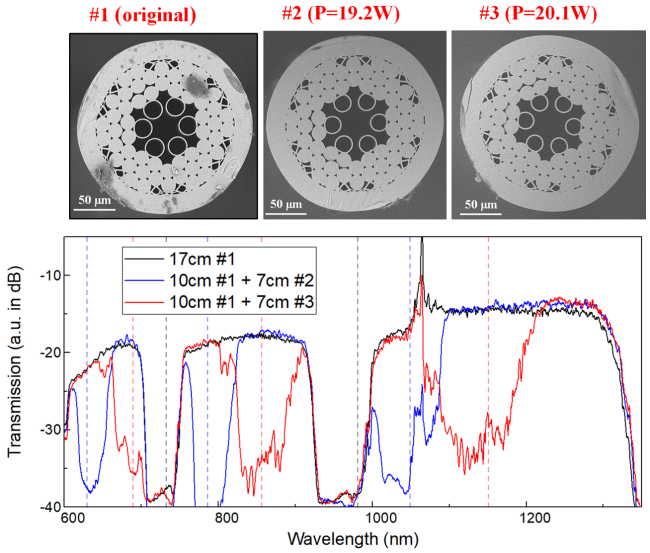

Figure 4. Transmission spectra of different fiber combinations. Fiber #1: unprocessed fiber, $t = 1.40$ μm, $D = 31.2$ μm; Fiber #2: processed under $P = 19.2$ W, $t = 1.49$ μm, $D = 33.2$ μm; Fiber #3: processed under $P = 20.1$ W, $t = 1.63$ μm, $D = 36.5$ μm. Resonant wavelengths of Fiber #1, Fiber #2 and Fiber #3 are calculated from Equation (1) and marked with dashed black lines, dashed blue lines and dashed red lines respectively.

More interestingly, as both t and D were changed, the dispersion curve of the fiber significantly shifted. As shown in Figure 5a, the Effective Refractive Index (ERI) curves were obtained by fitting the simulation values (solid dots), then the Group Velocity Dispersion (GVD) curves were calculated from the ERI curves, as shown in Figure 5b. As the fiber structure was changed from #1–#3, the zero dispersion wavelength shifted from around 860 nm to around 1000 nm. The change of the core size was responsible for this dispersion curve transformation [4]. Therefore, the proposed method also has promising prospects in applications relying on dispersion control, especially in pulse compression.

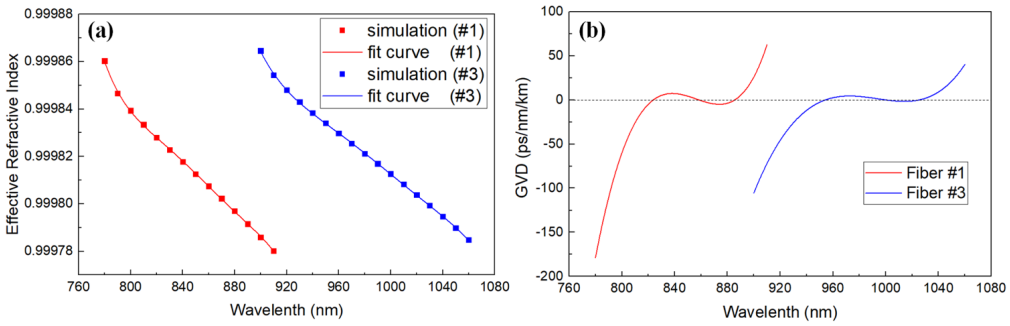

Figure 5. (**a**) Effective refractive index and (**b**) GVD (Group Velocity Dispersion) curve of both Fiber #1 and #3. In (**a**), the dots plot the simulation values, while the solid curves are quintic functions, which fit the simulation values.

The method is also applicable to a multiple layer HC-ARF, as evidenced by the results in Figure 6. The two-layer structure responded to the CO_2 laser writing process to introduce an additional rejection band. As indicated in both Figures 4 and 6, implementing a new single different wall thickness for an existing HC-ARF can made band reject filters. Here, we also demonstrate a band pass filter by introducing multiple different wall thicknesses into an original HC-ARF. The procedure is described in Figure 7. We used a two-layer HC-ARF as a pristine fiber. A section of 7 cm in the 25 cm-long pristine fiber (Fiber #4) was written under exposure power P = 19.4 W. Its corresponding transmission is present in the blue curve in Figure 7. Subsequently, another section of the same length was written by the lower power of P = 18.7 W to decrease the number of transmission bands (red line in Figure 7). The final fiber had limited transmission bands and worked more like a band pass filter with low excess loss, but 20-dB high extinction ratio.

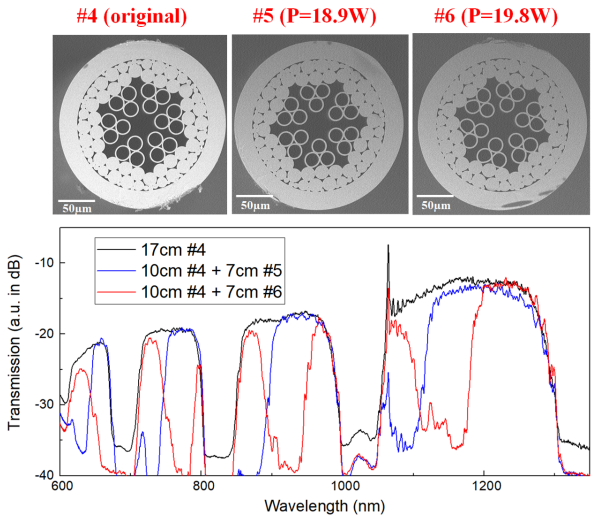

Figure 6. Transmission spectra of different fiber combinations. Fiber #4: unprocessed fiber, t = 1.97 μm; Fiber #5: processed under P = 18.9 W, t = 2.09 μm; Fiber #6: processed under P = 19.8 W, t = 2.21 μm.

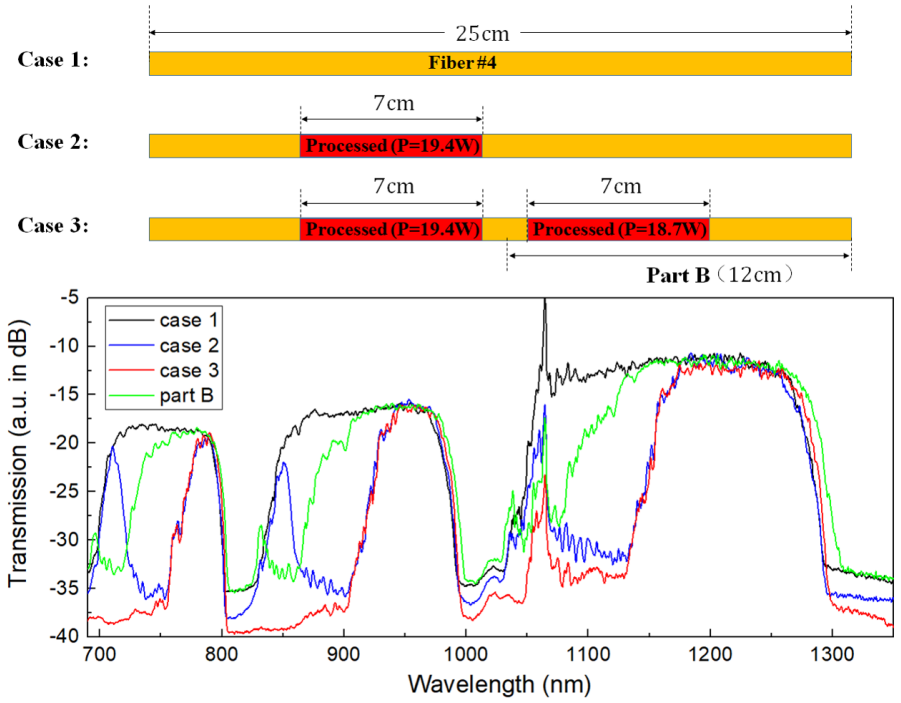

Figure 7. Schematic diagram illustrating the steps to make an HC-ARF-based band pass filter. As multiple different wall thicknesses are "written" into the original HC-ARF, the transmission bands are greatly narrowed.

The demonstrated HC-ARF-based filter could find interesting applications such as pump and signal wavelength separation in a gas-/liquid-filled HC-ARF system. HC-ARFs have been adopted to demonstrate excellent cavities for gas Raman generation and optofluidic systems [19,20] in which for both cases, free space optical filters were selected to filter out the excitation beam. Alternatively, by simply processing the HC-ARF with the method proposed in this work, an HC-ARF-based optical filter can be seamlessly written into the system without extra loss, as illustrated in Figure 8. This would be one step closer to an all-fiberized hollow core fiber system.

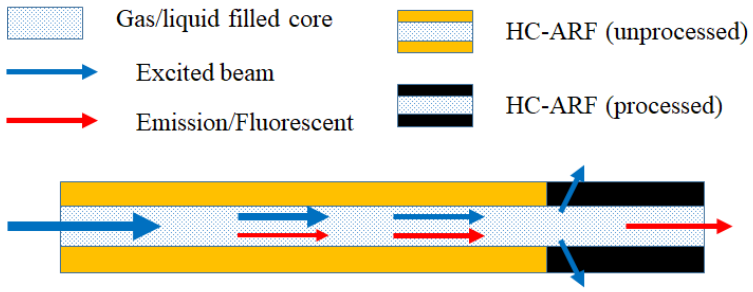

Figure 8. This schematic diagram shows the working principle of the HC-ARF-based filter in gas-/liquid-filled optical systems.

4. Conclusions

HC-ARFs with uniform wall thickness thave multiple and broad transmission bands. We have shown that writing a different wall thickness HC-ARF is feasible by using a CO_2 laser-based glass process stage. Consequently, the written HC-ARF exhibits the AND operation of two transmission characteristics defined by the written and the pristine HC-ARFs' wall thicknesses. In addition, we demonstrated multiple chained AND operations by writing various wall thickness HC-ARFs

in series along the fiber axis. On the basis of this principle, a novel method has also been proposed and demonstrated to convert HC-ARFs into in-fiber filters. The HC-ARF filter fabricated by this method benefits from low excess loss, easy integration with the HC-ARF-based system and controllable transmission/rejection wavelengths. We have also suggested a potential application of such fiber filters toward an all-fiberized HC-ARF system.

Author Contributions: X.H. conceived of the idea, performed the experiments, analyzed the data and wrote the manuscript. S.Y. supervised the design of the study and revised the manuscript. K.-T.Y supervised the design and participated in the experimental setup.

Funding: This research received no external funding.

Acknowledgments: S.Y. acknowledges support from KEIP through the Global Research Programme.

Conflicts of Interest: The authors declare no conflict of interest.

Abbreviations

The following abbreviations are used in this manuscript:

HC-PCF	Hollow-Core Photonic Crystal Fiber
HC-PBGF	Hollow-Core Photonic Bandgap Fiber
HC-ARF	Hollow-Core Anti-Resonant Fiber
ERI	Effective Refractive Index
GVD	Group Velocity Dispersion

References

1. Birks, T.A.; Roberts, P.J.; Russell, P.S.J.; Atkin, D.M.; Shepherd, T.J. Full 2-D photonic bandgaps in silica/air structures. *Electron. Lett.* **1995**, *31*, 1941–1943.:19951306. [CrossRef]
2. Smith, C.M.; Venkataraman, N.; Gallagher, M.T.; Müller, D.; West, J.A.; Borrelli, N.F.; Allan, D.C.; Koch, K.W. Low-loss hollow-core silica/air photonic bandgap fibre. *Nature* **2003**, *424*, 657–659. [CrossRef] [PubMed]
3. Jaworski, P.; Yu, F.; Carter, R.M.; Knight, J.C.; Shephard, J.D.; Hand, D.P. High energy green nanosecond and picosecond pulse delivery through a negative curvature fiber for precision micro-machining. *Opt. Express* **2015**, *23*, 8498–8506. [CrossRef] [PubMed]
4. Gérôme, F.; Cook, K.; George, A.K.; Wadsworth, W.J.; Knight, J.C. Delivery of sub-100fs pulses through 8 m of hollow-core fiber using soliton compression. *Opt. Express* **2007**, *15*, 7126–7131. [CrossRef] [PubMed]
5. Poletti, F.; Wheeler, N.V.; Petrovich, M.N.; Baddela, N.; Fokoua, E.N.; Hayes, J.R.; Gray, D.R.; Li, Z.; Slavík, R.; Richardson, D.J. Towards high-capacity fibre-optic communications at the speed of light in vacuum. *Nat. Photonics* **2013**, *7*, 279–284. [CrossRef]
6. Roberts, P.J.; Couny, F.; Sabert, H.; Mangan, B.J.; Williams, D.P.; Farr, L.; Mason, M.W.; Tomlinson, A.; Birks, T.A.; Knight, J.C.; et al. Ultimate low loss of hollow-core photonic crystal fibres. *Opt. Express* **2005**, *13*, 236–244. [CrossRef] [PubMed]
7. Couny, F.; Benabid, F.; Roberts, P.J.; Light, P.S.; Raymer, M.G. Generation and photonic guidance of multi-octave opticalfrequency combs. *Science* **2007**, *318*, 1118–1121. [CrossRef] [PubMed]
8. Gao, S.F.; Wang, Y.Y.; Ding, W.; Jiang, D.L.; Gu, S.; Zhang, X.; Wang, P. Hollow-core conjoined-tube negative-curvature fibre with ultralow loss. *Nat. Common.* **2018**, *9*, 2828–2828. [CrossRef] [PubMed]
9. Huang, X.; Yoo, S.; Yong, K. Function of second cladding layer in hollow core tube lattice fibers. *Sci. Rep.* **2017**, *7*, 1618. [CrossRef] [PubMed]
10. Poletti, F. Nested anti-resonant nodeless hollow core fiber. *Opt. Express* **2014**, *22*, 23807–23828. [CrossRef] [PubMed]
11. Yu, F.; Knight, J.C. Negative curvature hollow core optical fiber. *IEEE J. Sel. Top. Quantum Electron.* **2016**, *22*, 4400610. [CrossRef]
12. Huang, X.; Qi, W.; Ho, D.; Yong, K.T.; Luan, F.; Yoo, S. Hollow core anti-resonant fiber with split cladding. *Opt. Express* **2016**, *24*, 7670–7678. [CrossRef] [PubMed]
13. Belardi, W.; Knight, J.C. Effect of core boundary curvature on the confinement losses of hollow anti-resonant fibers. *Opt. Express* **2013**, *21*, 21912–21917. [CrossRef] [PubMed]

14. Hayes, J.R.; Sandoghchi, S.R.; Bradley, T.D.; Liu, Z.; Slavík, R.; Gouveia, M.A.; Wheeler, N.V.; Jasion, G.; Chen, Y.; Fokoua, E.N.; et al. Antiresonant hollow core fiber with an octave spanning bandwidth for short haul data communications. *J. Lightwave Technol.* **2017**, *35*, 437–442. [CrossRef]
15. Debord, B.; Amsanpally, A.; Chafer, M.; Baz, A.; Maurel, M.; Blondy, J.; Hugonnot, E.; Scol, F.; Vincetti, L.; Gérôme, F.; et al. Ultralow transmission loss in inhibited-coupling guiding hollow fibers. *Optica* **2017**, *4*, 209–217. [CrossRef]
16. Belardi, W.; Knight, J.C. Hollow anti-resonant fibers with reduced attenuation. *Opt. Lett.* **2014**, *39*, 1853–1856. [CrossRef] [PubMed]
17. Gao, S.F.; Wang, Y.Y.; Ding, W.; Wang, P. Hollow-core negative-curvature fiber for UV guidance. *Opt. Lett.* **2018**, *43*, 1347–1350. [CrossRef] [PubMed]
18. Yu, F.; Wadsworth, W.J.; Knight, J.C. Low loss silica hollow core fibers for 3–4 μm spectral region. *Opt. Express* **2012**, *20*, 11153–11158. [CrossRef] [PubMed]
19. Liu, X.L.; Ding, W.; Wang, Y.Y.; Gao, S.F.; Cao, L.; Feng, X.; Wang, P. Characterization of a liquid-filled nodeless anti-resonant fiber for biochemical sensing. *Opt. Lett.* **2012**, *42*, 863–866. [CrossRef] [PubMed]
20. Williams, G.O.; Euser, T.G.; Arlt, J.; Russell, P.S.J.; Jones, A.C. Hollow anti-resonant fibers with reduced attenuation. *ACS Photonics* **2014**, *1*, 790–793. [CrossRef]
21. Russell, P.S.J.; Hölzer, P.; Chang, W.; Abdolvand, A.; Travers, J.C. Hollow-core photonic crystal fibres for gas-based nonlinear optics. *Nat. Photonics* **2014**, *8*, 278–286. [CrossRef]
22. Huang, X.; Ma, J.; Tang, D.; Yoo, S. Hollow-core air-gap anti-resonant fiber couplers. *Opt. Express* **2017**, *25*, 29296–29306. [CrossRef]
23. Liu, X.; Fan, Z.; Shi, Z.; Ma, Y.; Yu, J.; Zhang, J. Dual-core anti-resonant hollow core fibers. *Opt. Express* **2016**, *24*, 17453–17458. [CrossRef] [PubMed]
24. Argyros, A.; Leon-Saval, S.G.; van Eijkelenborg, M.A. Twin-hollow-core optical fibres. *Opt. Commun.* **2009**, *282*, 1785–1788. [CrossRef]
25. Ouellette, F. All-fiber filter for efficient dispersion compensation. *Opt. Lett.* **1991**, *16*, 303–305. [CrossRef] [PubMed]
26. Antonio-Lopez, J.E.; Castillo-Guzman, A.; May-Arrioja, D.A.; Selvas-Aguilar, R.; LiKamWa, P. Tunable multimode-interference bandpass fiber filter. *Opt. Lett.* **2010**, *35*, 324–326. [CrossRef] [PubMed]
27. Pryamikov, A.D.; Biriukov, A.S.; Kosolapov, A.F.; Plotnichenko, V.G.; Semjonov, S.L.; Dianov, E.M. Demonstration of a waveguide regime for a silica hollow-core microstructured optical fiber with a negative curvature of the core boundary in the spectral region >3.5 μm. *Opt. Express* **2011**, *19*, 1441–1448. [CrossRef] [PubMed]
28. Kolyadin, A.N.; Kosolapov, A.F.; Pryamikov, A.D.; Biriukov, A.S.; Plotnichenko, V.G.; Dianov, E.M. Light transmission in negative curvature hollow core fiber in extremely high material loss region. *Opt. Express* **2013**, *21*, 9514–9519. [CrossRef] [PubMed]
29. KolBrilland, L.; Smektala, F.; Renversez, G.; Chartier, T.; Troles, J.; Nguyen, T.N.; Traynor, N.; Monteville, A. Fabrication of complex structures of Holey Fibers in Chalcogenide glass. *Opt. Express* **2006**, *14*, 1280–1285. [CrossRef]
30. Litchinitser, N.M.; Dunn, S.C.; Usner, B.; Eggleton, B.J.; White, T.P.; McPhedran, R.C.; de Sterke, C.M. Resonances in microstructured optical waveguides. *Opt. Express* **2003**, *11*, 1243–1251. [CrossRef] [PubMed]
31. Issa, N.A.; Poladian, L. Vector wave expansion method for leaky modes of microstructured optical fibers. *J. Lightwave Technol.* **2003**, *21*, 1005–1012. [CrossRef]